



# A first step towards a consensus static *in vitro* model for simulating full-term infant digestion



O. Ménard<sup>a</sup>, C. Bourlieu<sup>a</sup>, S.C. De Oliveira<sup>a</sup>, N. Dellarosa<sup>b</sup>, L. Laghi<sup>b</sup>, F. Carrière<sup>c</sup>, F. Capozzi<sup>b</sup>, D. Dupont<sup>a</sup>, A. Deglaire<sup>a,\*</sup>

<sup>a</sup> STLO, UMR 1253, INRA, Agrocampus Ouest, Rennes, France

<sup>b</sup> Department of Agricultural and Food Sciences, University of Bologna, Cesena, Italy

<sup>c</sup> CNRS, Aix Marseille Université, UMR7282 Enzymologie Interfaciale et Physiologie de la Lipolyse, Marseille, France

## ARTICLE INFO

### Keywords:

Infant  
Digestion  
Static  
Model  
Infant formula

## ABSTRACT

*In vitro* alternatives to clinical trials are used for studying human food digestion. For simulating infant digestion, only a few models, lacking physiological relevance, are available. Thanks to an extensive literature review of the *in vivo* infant digestive conditions, a gastrointestinal static *in vitro* model was developed for infants born at term and aged 28 days. The model was applied to the digestion of a commercial infant formula. Kinetics of digestion, as well as the structural evolution, were compared with those obtained while submitting the same formula to the adult international consensus protocol of *in vitro* static digestion. The kinetics of proteolysis and lipolysis differed according to the physiological stage resulting mainly from the reduced level of enzymes and bile salts, as well as the higher gastric pH in the infant model. This *in vitro* static model of infant digestion is of interest for scientists, food or pharmaceutical manufacturers.

## 1. Introduction

The study of digestion is difficult to conduct in humans as *in vivo* trials imply technical, ethical and financial constraints. *In vitro* alternatives thus need to be developed for a better understanding of digestive kinetics. *In vitro* models allow the screening of various foods, before conducting *in vivo* animal or human trials on a limited number of food matrices. Whereas an international consensus has recently been found for mimicking digestion at the adult stage with an *in vitro* static model (Minekus et al., 2014), there is no physiologically-relevant harmonized model of *in vitro* static digestion at the infant stage (Shani-Levi et al., 2017). Previous reviews have compiled the physiological data available about infant digestive conditions (Abrahamse et al., 2012; Bourlieu et al., 2014), underlining the immaturity of the infant digestive system compared to the adult one. This immaturity concerns both enzymatic (type of enzymes and level of activity) and non-enzymatic (milk-based diet, frequency of feeding, bile salts concentrations) parameters.

The importance of the early infancy period in terms of nutrition and of preprogramming concept is now widely acknowledged. Using adequate *in vitro* digestion tools is a priority for optimizing infant formula. The quantity of recent publications presenting results of *in vitro* infant digestion is a good illustration of the interest towards this tool, such as reviewed recently (Shani-Levi et al., 2017). Digestion models can be

static (Dupont et al., 2010), semi-dynamic (Amara et al., 2014; Bourlieu et al., 2015) or dynamic (Blanquet et al., 2004; de Oliveira et al., 2016). Focusing on static models, a recent review has highlighted the variability in the parameters used to mimic infant digestion (Shani-Levi et al., 2017). In particular, the enzymatic parameters are scarcely expressed in international units (I.U.) and experimental enzyme characterization is most of the time omitted, which makes the comparison of the results among studies difficult. Thus, a detailed *in vitro* digestion model based on *in vivo* digestive parameters of neonates is needed. In this context, the aim of the present study was to firstly propose an *in vitro* static digestion model for the full-term newborn (28 days of life, gestation age from 38 to 42 wk) with parameters relying on *in vivo* data published in the literature, and secondly to compare this infant model with the adult international consensus model in regards to the digestive kinetics of the same food, *i.e.* a commercial infant formula.

## 2. Materials & methods

### 2.1. Meal

A commercial liquid infant formula for infants from birth to 6 months was bought in a local supermarket. The formula was composed of 1.18 g of proteins (ratio casein/whey protein w/w: 30/70) and

\* Corresponding author at: UMR 1253 Science et Technologie du Lait et de l'oeuf, 65 rue de St Briec, 35042 Rennes Cedex, France.  
E-mail address: [amelie.deglaire@agrocampus-ouest.fr](mailto:amelie.deglaire@agrocampus-ouest.fr) (A. Deglaire).

3.45 g of lipids (43% of saturated fatty acids) for 100 ml of formula, as measured by the Kjeldhal method and the acido-butyrometric method, respectively. A content of 7.5 g of carbohydrates for 100 ml of formula was labelled.

## 2.2. Chemicals and enzymes

Materials were all standard analytical grade. Chemicals, enzymes and bile were purchased from Sigma Aldrich (Saint Quentin Fallavier, France). Pepsin (Sigma P6887) and pancreatin (Sigma, P7545 8XUSP) were of porcine origin while bile (Sigma B8631) was of bovine origin. Rabbit gastric extract (RGE) was provided by Lipolytech (Marseille, France). Enzyme activities were determined as described in the Electronic Supplementary Information of Minekus et al. (2014).

## 2.3. In vitro digestion protocol

### 2.3.1. Infant model

The infant gastrointestinal static *in vitro* model was set up in order to mimic as close as possible the digestive conditions of full-term infants. Parameters were defined thanks to the extensive literature review of the *in vivo* infant digestive conditions previously conducted within our laboratory (Bourlieu et al., 2014).

The infant food is liquid and its time of residence in the mouth is short. Considering this, the oral phase was omitted, such as suggested for the adult international consensus (Minekus et al., 2014). The static *in vitro* digestion model proposed here included two consecutive steps: a gastric and an intestinal phase. The full-term infant digestive parameters of the present model are summarized in Fig. 1.

**2.3.1.1. Gastric phase.** Parameters (meal to secretions ratio, pH) were determined based on the infant gastric conditions occurring at the emptying half-time, assumed to be more representative than the final time point. As described by Bourlieu et al. (2014), a gastric emptying half-time of 78 min has been reported for infant formula. The meal to secretions ratio was based on the simulation of secretion flows in the dynamic digestion model DIDGI® validated for infant formula digestion (Ménard et al., 2014), where the mean flow rate of secretions was fixed at 0.53 ml/min. At 78 min after the start of the meal ingestion, the ratio (v/v) of meal to secretions was 63 to 37.

Compilation of data measuring gastric pH in infants allowed the determination of a linear regression describing the gastric acidification curve:  $\text{pH} = -0.015 \cdot \text{time (min)} + 6.52$ , as previously described (Bourlieu et al., 2014). Considering the gastric emptying half-time of 78 min, gastric pH in the static model was set up at 5.3.

Based on postprandial enzyme activities determined in infant gastric aspirates, average values of 63 U of pepsin and 4.5 U of lipase per ml of gastric content and per kg of body weight of infant (Armand et al., 1996; Roman et al., 2007) were found. Thus, considering the mean body weight of a one-month old infant of 4.25 kg (de Oliveira et al., 2016), enzyme activities were set up at 268 U/ml of gastric content for pepsin and 19 U/ml of gastric content for lipase. Pepsin and gastric lipase were added as rabbit gastric extract (RGE). Rabbit gastric lipase presents 85% of sequence homology as compared to the human one (Roussel et al., 1999). The added amount of RGE covered 100% of the pepsin activity and 110% of the lipase activity required (21 U/ml).

Gastric fluid composition was based on a study on 30 full-term infants reported by Hyde (1968). The simulated gastric fluid (SGF) was composed of sodium chloride and potassium chloride fixed at 94 and 13 mM, respectively, and adjusted to pH 5.3 with HCl 1 M. After 60 min of gastric digestion, the pH was increased to 7 by addition of NaOH 1 M in order to stop gastric enzyme activities before further intestinal digestion.

**2.3.1.2. Intestinal phase.** The previous vial containing the 60 min gastric phase was adjusted to the intestinal pH of 6.6 using HCl 1 M. As for the gastric phase, the meal to secretions ratio for the intestinal phase was determined at 78 min of digestion using the simulation of secretion flows (bile, pancreatin and sodium bicarbonate) in the dynamic digestion model DIDGI® (Ménard et al., 2014), where the overall mean secretion flow rate was 0.85 ml/min. Thus, at 78 min of digestion, the ratio (v/v) meal to total secretion (gastric and intestinal) for the intestinal phase was 39 to 61. More precisely, the total volume of the intestinal phase was composed of 39% of meal, 23% of gastric secretion and 38% of intestinal secretion.

The simulated intestinal fluid (SIF), based on the characterization of duodenal fluid of 1-week-old full-term infants (Zoppi, Andreotti, Pajno-Ferrara, Bellini, & Gaburro, 1973), was composed of 164 mM of sodium chloride, 10 mM of potassium chloride and 85 mM of sodium bicarbonate and adjusted at pH 7. Calcium chloride was added separately before the beginning of the intestinal phase at a concentration of 3 mM within the volume of the intestinal fluid (Zoppi et al., 1973). Bovine bile extract was added to a final content of 3.1 mM of bile salts, which corresponds to the average postprandial value determined in duodenal aspirates of eight 2-week-old infants (Signer, Murphy, Edkins, & Anderson, 1974).

The added amount of pancreatin covered the intestinal lipase activity required of 90 U/ml of intestinal content (Norman, Strandvik, & Ojamae, 1972) and the trypsin activity needed i.e. 16 U/ml of intestinal content, which was consistent with previously reviewed *in*

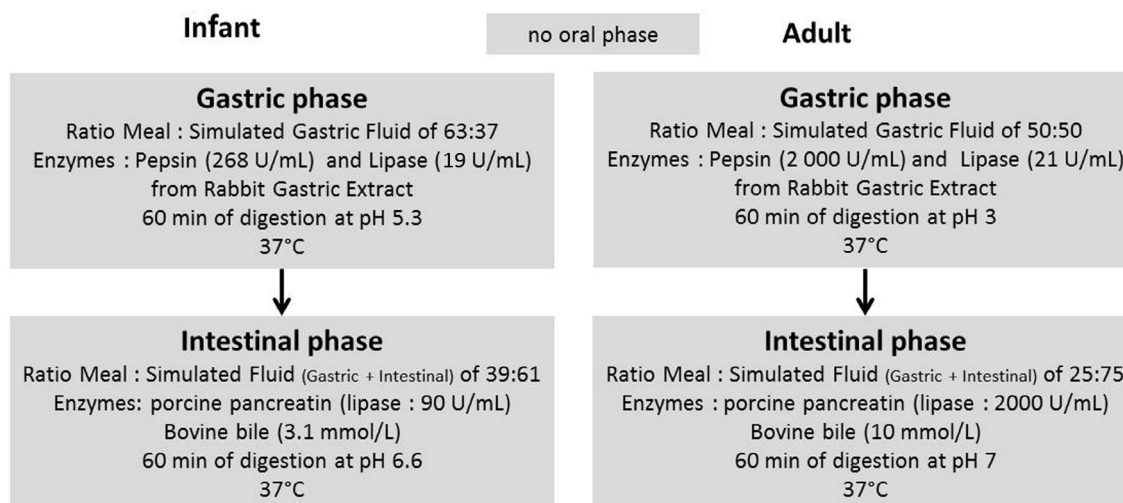


Fig. 1. Infant and adult digestive conditions used in the static *in vitro* digestion models.

*vivo* data (Poquet & Wooster, 2016).

### 2.3.2. Adult model

The adult international consensus protocol of *in vitro* static digestion (Minekus et al., 2014) was adapted to our liquid infant formula. The oral phase was omitted such as for the infant model. The same sources of enzymes as those for the infant model were used and their concentrations were adjusted to the recommended levels, as described in Minekus et al. (2014). For the gastric phase, a combination of two pepsin origins (RGE and porcine pepsin) covered the required pepsin activity, which is higher in adults than in infants. The gastric lipase level that is supposed to be mature at birth was similar in both adult and infant models. In the intestinal phase, porcine pancreatin and bovine bile were added to cover the required level, as summarized in Fig. 1.

For the infant and adult models, gastric and intestinal steps lasted 60 min each, and were performed at 37 °C in a shaking water bath (50 rpm). Each gastrointestinal digestion was conducted in triplicate.

## 2.4. Meal and digesta characterization

In both adult and infant digestion assays, gastric and intestinal digesta were sampled after 5, 15, 30 and 60 min of digestion. Particle size measurements and microscopic observations were performed on the infant formula prior to digestion and at the endpoint of the gastric step (G60) on two out of the three infant or adult digestions. Other aliquots were either used directly for lipid extraction or frozen (−20 °C) after addition of protease inhibitors i.e. 10 µl of Pepstatin A (0.72 µM) per ml of gastric digesta or 50 µl of Pefabloc (0.1 M) per ml of intestinal digesta.

### 2.4.1. Structural characterization

**2.4.1.1. Particle size measurements.** The particle size distributions were measured by laser light scattering using a Mastersizer 2000 (Malvern Instruments, Malvern, UK), with two laser sources. The refractive indexes used were 1.462 for vegetable oil at 633 and 466 nm and 1.333 for water (dispersant solution in the measurement cell). Samples were added to the measurement cell of the apparatus in order to reach 7–10% of obscuration. Samples were added either as is or after a 10-fold dilution in sodium dodecyl sulfate (SDS) to evaluate whether some aggregation occurred in the sample.

From the size distribution, the diameter mode (the population of the particles the most frequent in the volume distribution) and the diameter  $D[4,3]$  (the volume weighted mean diameter) were calculated.

**2.4.1.2. Confocal laser scanning microscopy (CLSM).** Microstructure was observed using a Nikon C1Si Laser Scanning Confocal Imaging System on an inverted microscope TE2000-E (Nikon, Champigny-sur-Marne, France) operated with an argon laser (excitation at 488 nm) and two He-Ne lasers (excitation at 543 and 633 nm), as previously described by Bourlieu et al. (2015) except that a 40-X oil-immersion objective was used for all images. Three fluorescent dyes, Fast Green, Rd-DOPE® and LipidtoX®, were used to colour simultaneously protein, amphiphilic compounds and apolar lipids, respectively (Bourlieu et al., 2015).

### 2.4.2. Biochemical characterization

**2.4.2.1. Protein analyses.** SDS-PAGE was performed on meal and digesta samples using 4–12% polyacrylamide NuPAGE Novex bis-Tris 15-well precast gels (Invitrogen, Carlsbad, CA, USA). All samples were diluted with NuPAGE® LDS sample buffer and then treated with DL-dithiothreitol and deionized water. Ten µg of meal proteins was loaded into each well, thus taking into account the meal: secretion ratio in order to evaluate the sole impact of proteolysis. Mark 12 Unstained Standard (Invitrogen) was used as a molecular weight (Mw) marker. Gels were fixed in 30% (v/v) ethanol, 10% (v/v) acetic acid and 60% (v/v) deionized water and were rinsed in deionized water before

staining with Bio-Safe Coomassie stain (Bio-Rad Laboratories, France). Discoloration of gels was performed with water. Image analyses of gels were carried out using Image scanner III (GE Healthcare Europe GbmH, Velizy-Villacoublay, France). Densitometry on bands was performed by measuring their grey intensity using the software Image Quant TL™ (GE Healthcare Europe183 GbmH, Velizy-Villacoublay, France). This allowed a semi-quantitative analysis of the digesta.

**2.4.2.2. Nuclear magnetic resonance (NMR).** To analyze the amino acid fraction solubilized for each digestion step, digesta samples (1 ml) were thawed and centrifuged for 5 min at 18 630g to remove the particles of undigested material. A sample of 800 µl was taken from the lower phase and added to 800 µl of chloroform stabilized with ethanol, to obtain a defatted fraction. After vortex mixing, the water soluble fraction was separated and added to 100 µl of a D<sub>2</sub>O solution of 3-(trimethylsilyl)propionic-2,2,3,3-d<sub>4</sub> acid sodium salt (TSP) 10 mM set at pH 7.0 by means of a 100 mM phosphate buffer. All the samples were kept refrigerated during preparation and immediately analyzed by NMR, at 10 °C to avoid further modifications on proteins.

By following the protocol of Bordoni et al. (2011) and Laghi et al. (2013), two kinds of NMR spectra were registered on each sample, in order to focus on different characteristics of the molecules solubilized by digestion. All spectra were registered at 600 MHz, by means of a Bruker AVANCE III spectrometer (Bruker, Milan, Italy). The first increment of a NOESY spectrum was obtained as described by Alum et al. (2008), with spectral width of 12 ppm and number of acquired points equal to 32k, for an acquisition time of 2.28 s. Relaxation time, 90° pulse and number of scans were set to 5 s, 10.91 µs and 4, respectively. These spectra showed the signals of all hydrogen atoms (<sup>1</sup>H) contained in the studied solution. These spectra were therefore chosen because they represented a handy mean for relative quantification of all the water soluble organic molecules in the digesta, i.e. peptides and free amino acids.

Transverse relaxation time ( $T_2$ ) weighted spectra were obtained by including a CPMG (Carr-Purcell-Meiboom-Gill) filter (Meiboom & Gill, 1958) to a free induction decay (FID) sequence. The filter was made up of a train of 400 echoes separated by 800 µs, for a total time of 328 ms. Each acquisition parameter of the CPMG pulses sequence was obtained from NOESY experiment, with the exception of the acquisition and dummy scans, both set to 16. CPMG spectra allowed focusing on the protons of low weight molecules only, therefore giving a qualitative estimate of the lowest molecular weight fraction.

To specifically focus on the aliphatic and amidic portions of amino acids, the 0.400–1.058 ppm, and 8.000–8.800 ppm spectra regions respectively were observed.

The NOESY and  $T_2$  weighted spectra registered at each digestion step were normalized towards NOESY spectra at G0 for adults, by taking advantage of the principle of reciprocity (Hoult, 2011). For this purpose, the summed area of aliphatic, branched, aromatic and amidic spectral regions were set to 100 arbitrary units.

**2.4.2.3. Lipid analysis.** Thin layer chromatography (TLC) was conducted to follow the evolution of the different lipid classes during lipolysis. Lipid extraction was performed on ice right after sampling based on the Folch method. Briefly, 400 µl of sample were added in 2.4 ml of chloroform/methanol (2:1 v:v) and acidified with 160 µl of HCl 0.1 N to stop lipolysis in the digesta. The extract was then rinsed with NaCl 0.73% (96 µl) and 600 µl of supplementary chloroform/methanol (2:1 v:v). The chloroform phase containing the lipid fraction was recovered and spotted on silica gel plates (10 × 20 cm, 0.25 mm, Si G60, Merck) using Automatic TLC Sampler III (CAMAG, Muttenz, Switzerland). In order to compare the extent of lipolysis between the two phases, the different meal to secretions ratio was taken into account in the volume spotted on TLC silica plates. Image analyses of the plates were performed as described for SDS-PAGE gels, allowing a semi-

quantitative analysis of the lipids.

**2.4.2.4. Free fatty acids.** Free Fatty Acids (FFA, C4:0 to C20:0) were analyzed by gas chromatography after lipid extraction, as described above, followed by a solid phase extraction (De Jong & Badings, 1990). Three internal standards (160  $\mu$ l of C5, C11 and C17 at 0.5 mg/ml) were added to each aliquot prior to its lipid extraction, as described by Bourlieu, Rousseau, Briard-Bion, Madec, and Bouhallab (2012). Samples were injected in triplicate. The relative contents of each FFA were converted into moles and reported to the total acyl chains in the undigested infant formula, which corresponded to the instantaneous lipolysis degree.

## 2.5. Statistics

Statistical analyses were conducted using the R software, version 3.1.2 (R Core Team, 2014). T-tests were conducted between the infant and adult models at each time of digestion. For data arising from SDS-PAGE and TLC, where one adult and one infant digestion samples were deposited on each gel or plate, data were considered as paired within each gel or plate. Data are presented as mean  $\pm$  SD.

## 3. Results

### 3.1. Proteolysis kinetics

The kinetics of proteolysis during adult and infant digestion are presented in Figs. 2 and 3. Digested samples from the gastric and intestinal phases were compared with the meal before digestion (G0) and allowed monitoring the proteolysis of the major proteins, *i.e.* caseins,  $\beta$ -lactoglobulin and  $\alpha$ -lactalbumin (Fig. 2). Caseins appeared to be drastically hydrolyzed at the adult stage within the first five minutes of gastric digestion (Fig. 2B), whereas, in the infant, caseins were gradually hydrolyzed up to a residual level of  $10.9 \pm 6.5\%$  at 60 min of gastric digestion (G60). Regarding  $\beta$ -lactoglobulin and  $\alpha$ -lactalbumin,

they were extensively hydrolyzed in the adult ( $11.5 \pm 3.3\%$  and  $3.7 \pm 1.0\%$  remaining at G60, respectively). In contrast, in the infant these whey proteins resisted to gastric digestion (Fig. 2C and D), with  $82.0 \pm 7.4\%$  and  $86.7 \pm 6.8\%$  of  $\beta$ -lactoglobulin and  $\alpha$ -lactalbumin remaining at G60, respectively.

Intestinal digestion resulted in an extensive and rapid hydrolysis of the proteins remaining after the gastric step, especially for infant digestion. After five minutes of intestinal digestion, no more intact protein remained (Fig. 2A). The bands visible on the SDS-PAGE gel corresponded to the proteins present in the pancreatin added in the intestinal phase, as shown in supplemental Fig. 1.

Products of proteolysis, such as peptides and free amino acids, could be followed thanks to NMR, as shown in Fig. 3. Data from the aliphatic region, shown in Fig. 3A, give the intensity of the molecules solubilized by digestion relative to the G0 step for adults (undigested IF). In the gastric step, a low evolution of the signal up to five minutes of digestion appeared for the adult digestion and remained almost stable until the end of the gastric phase. For the infant stage, an even lower evolution of the signal during the gastric step was found. In contrast, a drastic increase of peptides and amino acids appeared during the first five minutes of the intestinal digestion, mainly for the adult. Between five and sixty minutes of intestinal digestion, infant and adult digestions showed the same behaviour with no evolution of the signal.

The amidic protons located at the surface of a protein tend to exchange with water, thus reducing to zero their contribution to the NMR signal. Therefore, the contribution of amidic protons, shown in the lower part of Fig. 3A, allowed a qualitative estimation of the high molecular weight peptides solubilized by digestion. The contribution to the total digesta from amidic protons was one third of that from the aliphatic portion of amino acids. As each aliphatic group of amino acids was characterized by three protons, this suggested that most of the molecules solubilized by digestion both in adult and infant stages corresponded to high molecular weight peptides. This was confirmed by  $T_2$  weighted spectra focusing on small molecules giving rise to signals in the aliphatic region (Fig. 3B), whose area at G5 was one tenth of the one

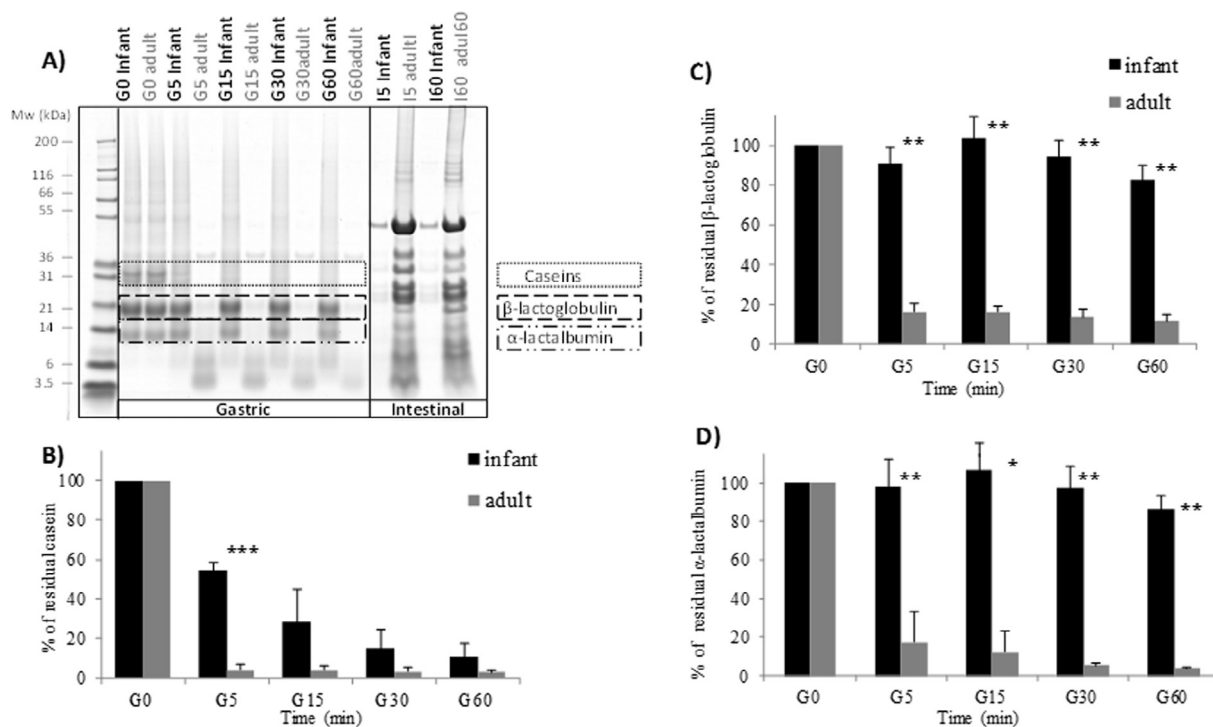


**Fig. 2.** SDS-PAGE protein profile comparing the *in vitro* static digestion of an infant formula at the infant or adult stages (example of a gel, A) and calculated percentage (%) of the residual intact proteins for B) casein, C)  $\beta$ -lactoglobulin and D)  $\alpha$ -lactalbumin during gastric digestion at the infant ( $n = 3$  digestions) or adult ( $n = 3$  digestions) stage. Data were obtained from densitometric analysis of the SDS-PAGE gels. (G: gastric phase, I: intestinal phase; the numbers represent the time in min after the start of the digestion). Statistical significance: \*,  $p < 0.05$ ; \*\*,  $p < 0.01$ ; \*\*\*,  $p < 0.001$ .



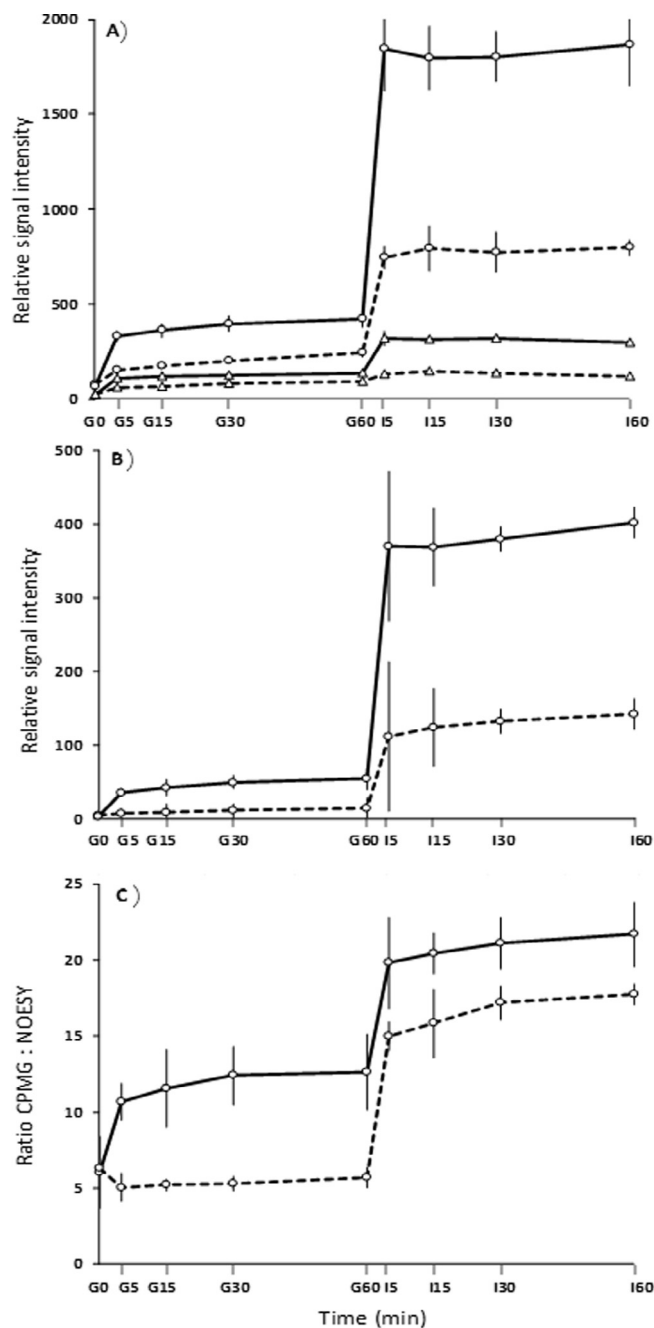


Fig. 3. Total signal from aliphatic (circle) and, when present, amidic (triangles) regions obtained from spectra registered by A) NOESY, B) CPMG or C) relative ratio CPMG: NOESY (%), during gastric (G) and intestinal (I) digestion at the infant (dashed lines,  $n = 3$  digestions) or adult (full lines,  $n = 3$  digestions) stage. Numbers represent the time in min after the start of digestion. T-tests were conducted at each time of digestion between the infant and the adult stage. Each time point differs significantly ( $P < 0.05$ ) between these stages, except at G0 and at I5, I15 and I60 for the ratio CPMG:NOESY.

registered with NOESY for adults, and as low as one-twentieth for infant.

The evolution trends of small molecular weight molecules relative to high molecular weight molecules solubilized by digestion can be better appreciated from the relative abundance between them, as highlighted in Fig. 3C. At G0, the signal from low molecular weight molecules was close to 5% for infants, and showed no variation along gastric digestion. In contrast, adults showed a similar relative abundance at G0, but a rapid increase to 11–12% was observed at the end of gastric digestion. The trend was then parallel for the infant and adult stages, with an abrupt increase from gastric to intestinal phases,

followed by a slight, steady increase along the intestinal digestion.

### 3.2. Lipolysis kinetics

The lipolysis products and the FFA release are visualized in Fig. 4A and B. Regarding gastric lipolysis, no evolution along the time and no difference between physiological stages were observed ( $p > 0.05$ , Fig. 4). In the intestinal phase, a great increase of FFA was observed in the first five minutes of digestion for both infant and adult stages, but the level of FFA was significantly higher in adult than in infant during all the intestinal digestion (Fig. 4B). The instantaneous lipolysis degree for the infant stage is shown in Fig. 5. While the lipolysis degree remained between  $4.6 \pm 0.4$  and  $7.2 \pm 0.8\%$  all over the gastric digestion, it increased sharply during the first 30 min of the intestinal digestion ( $46.2 \pm 3.6\%$ ) and reached  $53.8 \pm 2.2\%$  after 60 min. For the adult stage, the gastric lipolysis ranged from  $3.7 \pm 0.8$  up to  $10.0 \pm 2.6\%$  at 60 min of digestion. At each gastric digestion time, there was no significant difference ( $p > 0.05$ ) between the infant and adult stages. Regarding the adult intestinal lipolysis, the degree could not be directly calculated due to the formation of methyl ester of fatty acids. TLC of bile and pancreatin showed that their lipid fraction was composed of only cholesterol-derived compounds (bile salts) and phospholipids (supplemental Fig. 2).

### 3.3. Structural characterization during gastric digestion

Prior to digestion, the infant formula contained only submicron particles, likely casein micelles and fat droplets, with a mode of  $0.2 \mu\text{m}$  (Fig. 6). In Fig. 6A, the CLSM images showed less material and larger particles for the adult compared to the infant at 60 min of gastric digestion. The decomposition of these images showed co-localization of protein, apolar lipid and amphiphilic compounds in the aggregates formed (data not shown). The particle size distribution (Fig. 6B and C) indicated that aggregates had a similar mode in the infant and adult stages ( $17.5 \pm 0.2$  and  $19.6 \pm 0.3 \mu\text{m}$ , respectively), but the last 10% of the particles were smaller in the infant than in the adult, being above  $29 \mu\text{m}$  and  $52 \mu\text{m}$ , respectively. Similarly, D[4,3] was smaller in infants than in adults ( $18.7 \pm 0.3$  and  $29.0 \pm 4.8 \mu\text{m}$ , respectively). The addition of SDS completely dissolved the aggregates for the infant but only partially for the adult (Fig. 6B and C).

## 4. Discussion

### 4.1. General

The aim of this work was to design a new static *in vitro* model simulating the gastrointestinal digestion of an infant born at term. The comparison of the digestion of the same infant formula using the present model or the *in vitro* adult international consensus protocol confirmed the expected differences in terms of digestive kinetics and of structural disintegration caused by the immaturity of the infant digestive conditions.

### 4.2. Proteolysis

At the infant stage, the gastric proteolysis was slower and reached a lower degree of hydrolysis than at the adult stage. For example, 15% of whey proteins were hydrolyzed in an infant whereas this percentage reached 90% in an adult. The difference between stages is more likely due to the higher gastric pH in infants (5.3) compared to adults (3.0) rather than the reduced amount of pepsin (7.5 times less in the infant). Indeed, Dupont et al. (2010), observed similar gastric digestion of purified  $\beta$ -casein and  $\beta$ -lactoglobulin between the infant and adult despite a pepsin concentration that was eight times lower in the infant. pH was similar in both models (adult: 2.5; infant: 3.0), and corresponded to the range of pH (1.6 to 4) where pepsin activity is optimum,

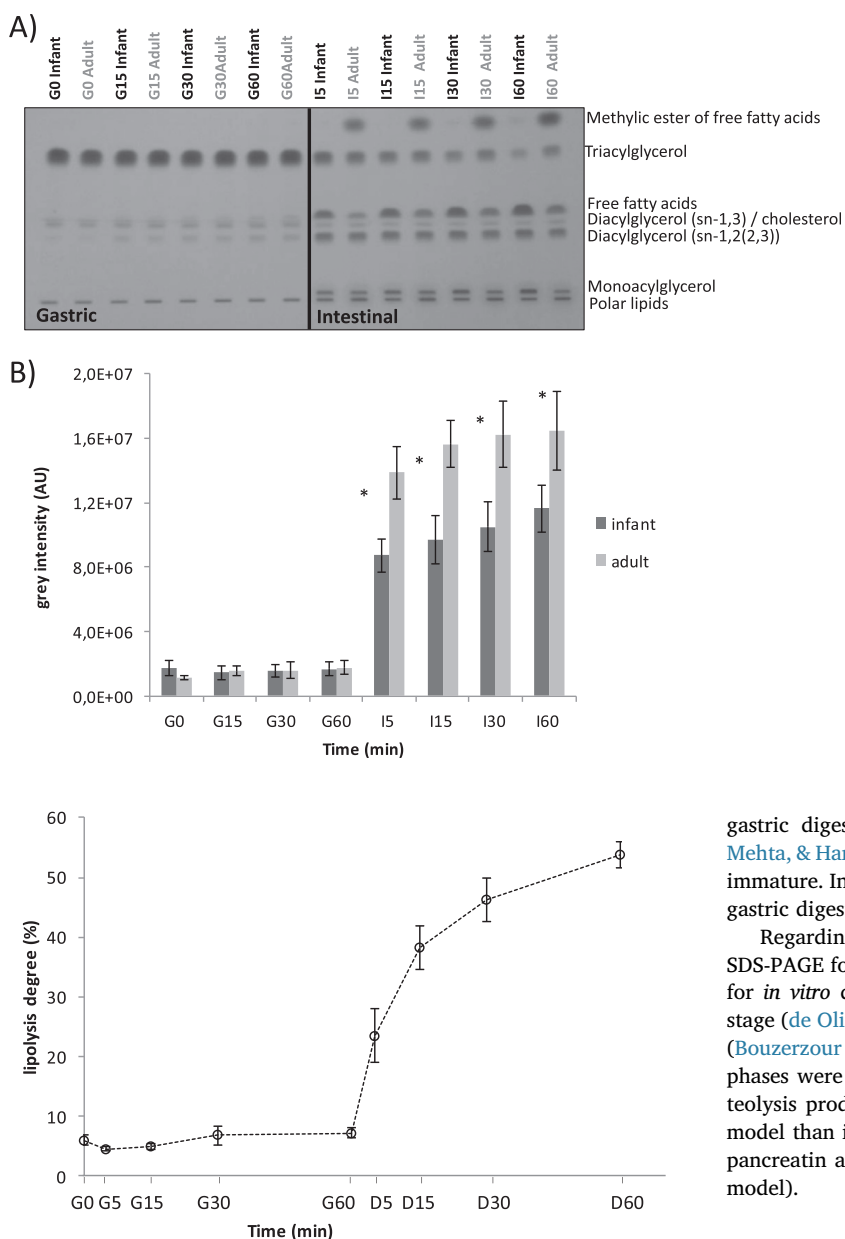


Fig. 5. Lipolysis degree during *in vitro* gastric and intestinal digestion of an infant formula at the infant stage ( $n = 3$  digestions) obtained by measuring fatty acids by gas chromatography (% of free fatty acids released from total esterified fatty acids in TAG).

i.e. with at least 70% of its maximal activity (Piper & Fenton, 1965). On the contrary, at a pH of 5.3 the pepsin activity should only be at 10% of its maximal activity (Piper & Fenton, 1965).

A different behaviour towards pepsinolysis has been highlighted in the present study between whey proteins that were shown to be resistant, and caseins shown to be more extensively hydrolyzed. This has been largely reported previously for bovine milk proteins in digestion studies conducted *in vitro* (Bourlieu et al., 2015; Dupont et al., 2010; Macierzanka, Sancho, Mills, Rigby, & Mackie, 2009) and *in vivo* in piglets (Bouzerzour et al., 2012) but also for human milk proteins ( $\alpha$ -lactalbumin vs. caseins) in preterm infants (de Oliveira et al., 2017). Caseins exhibit a loose and flexible structure that make them more susceptible to pepsinolysis than  $\beta$ -lactoglobulin and  $\alpha$ -lactalbumin, which have a globular and compact structure (Guo, Fox, Flynn, & Kindstedt, 1995). After 60 min of infant gastric digestion, 62% of intact proteins were estimated to remain. This may be compared with the *in vivo* value of 85% of intact proteins remaining after 50 min of

Fig. 4. Thin layer chromatography comparing the *in vitro* static digestion of an infant formula at the infant ( $n = 3$  digestions) or the adult ( $n = 3$  digestions) stages (example of a plate, A) and corresponding grey intensity (arbitrary unit, AU) of the free fatty acid released during digestion (B). Data obtained from densitometric analysis of the thin layer chromatography using silica plates. For the adult intestinal phase, intensity presented here arise from the sum of the intensity for the bands for free and methyl ester fatty acids. G: gastric phase, I: intestinal phase; the numbers represent the time in min after the start of the digestion. Statistical significance: \*,  $p < 0.05$ ; \*\*,  $p < 0.01$ ; \*\*\*,  $p < 0.001$ .

gastric digestion in preterm infants (Henderson, Hamosh, Armand, Mehta, & Hamosh, 2001), where digestive functions are even more immature. In the adult model, only 7% of intact proteins remained after gastric digestion.

Regarding intestinal proteolysis, no intact protein was detected by SDS-PAGE for both the infant and adult models, as previously observed for *in vitro* dynamic digestion of human milk at the full-term infant stage (de Oliveira et al., 2016) or for infant formula digestion in piglets (Bouzerzour et al., 2012). The protein bands visible in the intestinal phases were due to the pancreatic enzymes. The level of smaller proteolysis products determined by NMR, was much lower in the infant model than in the adult one probably because of the lower amount of pancreatin added in the infant model (22 times less than in the adult model).

#### 4.3. Lipolysis

The gastric lipolysis was relatively low and not significantly different between the stages, with  $7.2 \pm 0.8\%$  vs.  $10 \pm 2.6\%$  at 60 min of digestion in infants and adults, respectively (data not shown for adults). This can be explained by the same amount of gastric lipase included in both models, since full-term newborns are already mature for gastric lipase secretion. The different gastric pH for infants and adults did not seem to impact the lipolytic activity. Indeed, Moreau, Gargouri, Lecat, Junien, and Verger (1988a), Moreau, Gargouri, Lecat, Junien, and Verger (1988b) showed that for an emulsion of long-chain triacylglycerols containing 95% long-chain fatty acids ( $\geq C16$ ), like in the present infant formula, the rabbit gastric lipase exerted an optimum activity at pH 4, while releasing a limited amount of FFA at pH 3 and 5. The present values of gastric lipolysis are in line with previous results obtained during *in vitro* semi-dynamic digestion for a processed model infant formula, resulting in 8 to 10% of gastric lipolysis between 60 and 180 min of digestion (Bourlieu et al., 2015). The present values are also in the range of overall gastric lipolysis determined in preterm neonates for an infant formula, i.e. 6% at 60 min of digestion (Roman et al., 2007). However, Armand et al. (1996) determined a higher degree of overall lipolysis (14% at 50 min of digestion), which may arise from the

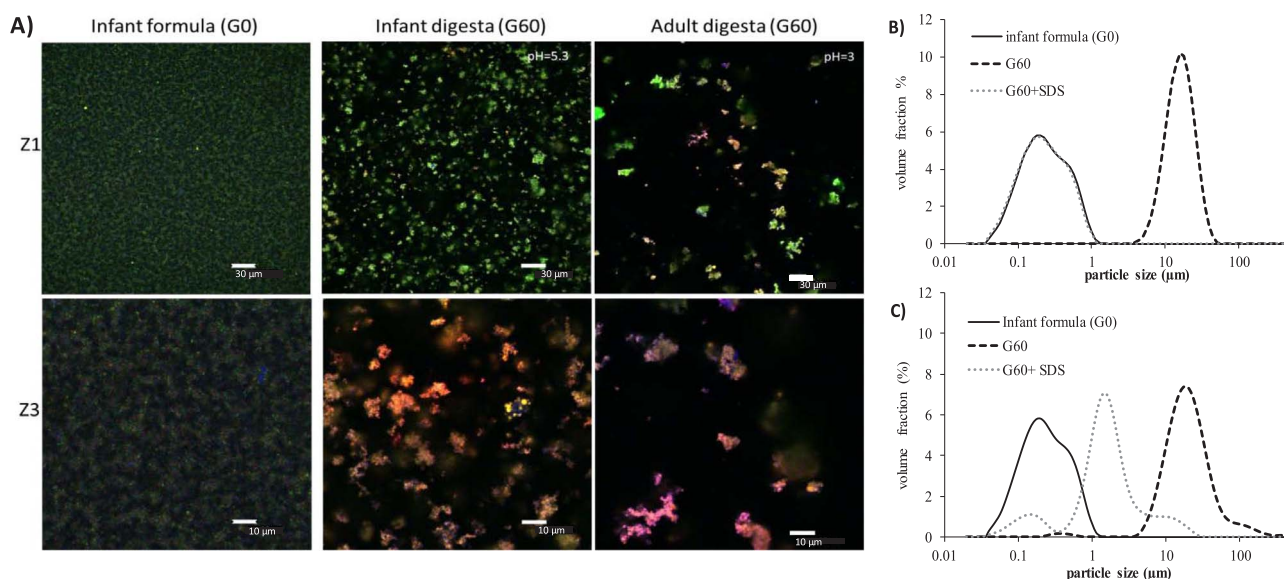


**Fig. 6.** A) Confocal laser scanning microscopy images (objective x40; zoom x1, Z1 or zoom x3, Z3) of an infant formula before digestion (G0) and at 60 min of gastric digestion (G60) at the infant or the adult stage (green: apolar lipids, red: polar lipids, blue: proteins) and corresponding mean particle size distributions with or without dissociating agent (SDS) B/ at the infant stage (n = 3 digestions) or C/ at the adult stage (n = 2 digestions). (For interpretation of the references to colour in this figure legend, the reader is referred to the web version of this article.)

different methods used to evaluate the overall lipolysis degree.

Regarding intestinal lipolysis, the lower level of FFA released during the infant digestion can be explained by the lower amounts of both intestinal lipase (22 times less in infant than in adult stage) and bio-surfactants, i.e. bile salts (3 times less in infant), reflecting the immaturity of the intestinal digestive function of the infant. The ratio between adult and infant intestinal lipase units used in the present study is consistent with a recent review (Poquet & Wooster, 2016), reporting values 10 to 20 times lower in infants than in adults. However, the ratio between infant and adult bile salt concentration may have been underestimated here, as there was 3 times more bile salts in the adult model compared to the infant one, while Poquet and Wooster (2016) have reported a ratio of 15. The degree of intestinal lipolysis in adults could not be determined due to the methyl esters of FFA formed during lipid extraction, not detectable by gas chromatography. These products derived from the reverse lipolysis reaction leading to the methyl esterification of free fatty acids (Supplemental Fig. 3).

#### 4.4. Relevance of the digestive parameters

The present model was based on the digestive parameters found at the gastric emptying half-time, which was an innovative and relevant strategy, more representative of the postprandial state as supported by the review of Sams, Paume, Giallo, and Carrière (2016) and Poquet and Wooster (2016). In the recent review of Shani-Levi et al. (2017), the comparison of eleven infant *in vitro* static digestion models showed that only 14% used a gastric pH  $\geq 5$  and 43% between pH 3 and 5. The other 43% used a gastric pH  $\leq 3$ , which is more representative of the fasting conditions.

Only a few digestion models include the use of a gastric lipase, either because only protein digestion is investigated but mainly because lipases that can be found commercially (microbial, fungal, animal or recombinant) often do not mimic the human gastric lipase (HGL) biochemical properties, i.e., *sn*-3 stereospecificity, stability and activity in a broad range of pH, resistance to pepsin and high tensioactivity (Bourlieu et al., 2012; Sams et al., 2016). On the contrary, rabbit gastric lipase used in the present study exhibits a high level of homology with HGL and leads to the same extent of lipolysis to that found *in vivo* (Poquet & Wooster, 2016; Sams et al., 2016); however, this lipase is not commercially available. Commercial availability of an affordable and

physiologically-relevant gastric lipase is a real need often pointed out by the scientific community working on food digestion.

The duration of each digestion step was set up at 60 min. Preliminary data based on 120 min of gastric digestion showed that this did not substantially impact the level of lipolysis and proteolysis observed by TLC and SDS-PAGE, respectively (data not shown). Regarding the intestinal phase, most of the hydrolysis occurred within the early time of intestinal digestion, and the evolution was slow within the last thirty minutes of digestion. Nevertheless, the duration of each phase may need to be extended or at least checked for other sources of proteins, such as plant proteins.

Regarding intestinal lipolysis, the major proportion of the FFA was released during the first five minutes and a slow increase of FFA was then observed during the remaining time. According to some authors (Hur, Lim, Decker, & McClements, 2011), adding calcium continuously and not as a single addition at the start of the digestion could avoid the enzymatic inhibition through FFA, by ionic complexation of FFA by calcium, but also possibly by limiting the precipitation of bile salts with calcium.

The present model could be extrapolated to older infants by considering the level of maturity of enzymes. In terms of gastric enzymes, Bourlieu et al. (2014) reported that gastric lipase was mature at birth for full-term infants, while for pepsin maturity increases progressively with age. Regarding the pancreatic lipases, the degree of maturity depends on the nature of the lipase, with the pancreatic lipase being almost completely immature and pancreatic lipase-related proteins (PLRP1, PLRP2) being mature (Yang, Sanchez, Figarella, & Lowe, 2000). While in adults the pancreatic lipase is responsible for the efficient intestinal digestion of dietary triglycerides (Carrière, Barrowman, Verger, & Laugier, 1993), in early life BSSL and PRPL2 have been presented as the major catalysts of fat digestion (Lindquist & Hernell, 2010). In the model proposed here, porcine pancreatic extract (pancreatin) has been added to cover the lipase activity required and contains both pancreatic lipase and carboxyl ester hydrolase (CEH; same enzyme as BSSL). So far, PLRP2 has not been identified in porcine pancreatic extracts, but since CEH/BSSL and PLRP2 share a similar substrate specificity (Bakala N'Goma, Amara, Dridi, Jannin, & Carrière, 2012), the use of pancreatin containing porcine CEH appears as relevant for infant digestion models.



## 5. Conclusion

The infant *in vitro* digestion model proposed in the present study takes into account the specificities of the gastrointestinal digestive conditions of full-term newborn infants, and represents a first step toward the establishment of a consensus static infant digestion model. Firstly, the comparison with the adult model highlighted the importance of taking into account the immaturity of the infant digestive conditions. Secondly, the comparison with *in vivo* data showed that this model is physiologically relevant. Thus, this is a new and simple tool that may help discriminating new infant formulas, differing by either composition, structure or process, but may also be useful to predict performance of oral drug delivery for newborns. This tool is thus of interest for scientists, food or pharmaceutical manufacturers, and can be a first step before preclinical studies.

## Conflicts of interest

The authors have declared no conflict of interest.

## Acknowledgements

This work was integrated in the COST action FA1005 INFOGEST on food digestion. The researchers associated in this cost action are acknowledged for contribution to the discussion on digestion parameters.

## Appendix A. Supplementary data

Supplementary data associated with this article can be found, in the online version, at <http://dx.doi.org/10.1016/j.foodchem.2017.07.145>.

## References

- Abrahamse, E., Minekus, M., van Aken, G. A., van de Heijning, B., Knol, J., Bartke, N., et al. (2012). Development of the digestive system-experimental challenges and approaches of infant lipid digestion. *Food Digestion*, 3(1–3), 63–77.
- Alum, M. F., Shaw, P. A., Sweatman, B. C., Ubhi, B. K., Haselden, J. N., & Connor, S. C. (2008). 4,4-dimethyl-4-silapentane-1-ammonium trifluoroacetate (dsa), a promising universal internal standard for nmr-based metabolic profiling studies of biofluids, including blood plasma and serum. *Metabolomics*, 4(2), 122–127.
- Amara, S., Patin, A., Giuffrida, F., Wooster, T. J., Thakkar, S. K., Benarouche, A., et al. (2014). *In vitro* digestion of citric acid esters of mono- and diglycerides (citrem) and citrem-containing infant formula/emulsions. *Food & Function*, 5(7), 1409–1421.
- Armand, M., Hamosh, M., Mehta, N. R., Angelus, P. A., Philpott, J. R., Henderson, T. R., et al. (1996). Effect of human milk or formula on gastric function and fat digestion in the premature infant. *Pediatric Research*, 40(3), 429–437.
- Bakala N'Goma, J. C., Amara, S., Dridi, K., Jannin, V., & Carrière, F. (2012). Understanding the lipid-digestion processes in the gi tract before designing lipid-based drug-delivery systems. *Therapeutic Delivery*, 3(1), 105–124.
- Blanquet, S., Zeijdner, E., Beyssac, E., Meunier, J. P., Denis, S., Havenaar, R., et al. (2004). A dynamic artificial gastrointestinal system for studying the behavior of orally administered drug dosage forms under various physiological conditions. *Pharmaceutical Research*, 21(4), 585–591.
- Bordoni, A., Picone, G., Babini, E., Vignali, M., Danesi, F., Valli, V., et al. (2011). Nmr comparison of *in vitro* digestion of parmigiano reggiano cheese aged 15 and 30 months. *Magnetic Resonance in Chemistry*, 49(S1), S61–S70.
- Bourlieu, C., Ménard, O., Bouzerzour, K., Mandalari, G., Macierzanka, A., Mackie, A. R., et al. (2014). Specificity of infant digestive conditions: Some clues for developing relevant *in vitro* models. *Critical Reviews in Food Science and Nutrition*, 54(11), 1427–1457.
- Bourlieu, C., Ménard, O., De La Chevasserie, A., Sams, L., Rousseau, F., Madec, M. N., et al. (2015). The structure of infant formulas impacts their lipolysis, proteolysis and disintegration during *in vitro* gastric digestion. *Food Chemistry*, 182, 224–235.
- Bourlieu, C., Rousseau, F., Briard-Bion, V., Madec, M. N., & Bouhallab, S. (2012). Hydrolysis of native milk fat globules by microbial lipases: Mechanisms and modulation of interfacial quality. *Food Research International*, 49(1), 533–544.
- Bouzerzour, K., Morgan, F., Cuinet, I., Bonhomme, C., Jardin, J., Le Huërou-Luron, I., et al. (2012). *In vivo* digestion of infant formula in piglets: Protein digestion kinetics and release of bioactive peptides. *British Journal of Nutrition*, 108(12), 2105–2114.
- Carrière, F., Barrowman, J. A., Verger, R., & Laugier, R. (1993). Secretion and contribution to lipolysis of gastric and pancreatic lipases during a test meal in humans. *Gastroenterology*, 105(3), 876–888.
- De Jong, C., & Badings, H. T. (1990). Determination of free fatty acids in milk and cheese. Procedures for extraction clean up and capillary gas chromatographic analysis. *Journal of High Resolution Chromatography*, 13, 94–98.
- de Oliveira, S. C., Bellanger, A., Ménard, O., Pladys, P., Le Gouar, Y., Dirson, E., et al. (2017). Impact of human milk pasteurization on gastric digestion in preterm infants: A randomized controlled trial. *The American Journal of Clinical Nutrition*.
- de Oliveira, S. C., Deglaire, A., Ménard, O., Bellanger, A., Rousseau, F., Henry, G., et al. (2016). Holder pasteurization impacts the proteolysis, lipolysis and disintegration of human milk under *in vitro* dynamic term newborn digestion. *Food Research International*, 88, 263–275.
- Dupont, D., Mandalari, G., Molle, D., Jardin, J., Leonil, J., Faulks, R. M., et al. (2010). Comparative resistance of food proteins to adult and infant *in vitro* digestion models. *Molecular Nutrition and Food Research*, 54(6), 767–780.
- Guo, M. R., Fox, P. F., Flynn, A., & Kindstedt, P. S. (1995). Susceptibility of beta-lactoglobulin and sodium caseinate to proteolysis by pepsin and trypsin. *Journal of Dairy Science*, 78(11), 2336–2344.
- Henderson, T. R., Hamosh, M., Armand, M., Mehta, N. R., & Hamosh, P. (2001). Gastric proteolysis in preterm infants fed mother's milk or formula. *Advances in Experimental Medicine and Biology*, 501, 403–408.
- Hoult, D. (2011). The principle of reciprocity. *Journal of Magnetic Resonance*, 213(2), 344–346.
- Hur, S. J., Lim, B. O., Decker, E. A., & McClements, D. J. (2011). *In vitro* human digestion models for food applications. *Food Chemistry*, 125(1), 1–12.
- Hyde, G. A. (1968). Gastric secretions following neonatal surgery. *Journal of Pediatric Surgery*, 3(6), 691–695.
- Laghi, L., Babini, E., Bordoni, A., Ciampa, A., Danesi, F., Di Nunzio, et al., (2013). Time domain measurements and high resolution spectroscopy are powerful nuclear magnetic resonance approaches suitable to evaluate the *in vitro* digestion of protein-rich food products. In: J. van Duynhoven, P. S. Belton, G. A. Webb & H. van As (Eds.), *Magnetic resonance in food science: Food for thought*, (pp. 235). Croydon, UK.
- Lindquist, S., & Hernell, O. (2010). Lipid digestion and absorption in early life: An update. *Current Opinion in Clinical Nutrition & Metabolism Care*, 13(3), 314–320.
- Macierzanka, A., Sancho, A. I., Mills, E. N. C., Rigby, N. M., & Mackie, A. R. (2009). Emulsification alters simulated gastrointestinal proteolysis of  $\beta$ -casein and  $\beta$ -lactoglobulin. *Soft Matter*, 5(3), 538.
- Meiboom, S., & Gill, D. (1958). Modified spin-echo method for measuring nuclear relaxation times. *Review of scientific instruments*, 29(8), 688–691.
- Ménard, O., Cattenoz, T., Guillemin, H., Souchon, I., Deglaire, A., Dupont, D., et al. (2014). Validation of a new *in vitro* dynamic system to simulate infant digestion. *Food Chemistry*, 145, 1039–1045.
- Minekus, M., Alminger, M., Alvito, P., Ballance, S., Bohn, T., Bourlieu, C., et al. (2014). A standardised static *in vitro* digestion method suitable for food – An international consensus. *Food & Function*, 5(6), 1113–1124.
- Moreau, H., Gargouri, Y., Lecat, D., Junien, J. L., & Verger, R. (1988a). Purification, characterization and kinetic properties of the rabbit gastric lipase. *Biochimica et Biophysica Acta*, 960(3), 286–293.
- Moreau, H., Gargouri, Y., Lecat, D., Junien, J. L., & Verger, R. (1988b). Screening of preduodenal lipases in several mammals. *Biochimica et Biophysica Acta*, 959(3), 247–252.
- Norman, A., Strandvik, B., & Ojamae, O. (1972). Bile acids and pancreatic enzymes during absorption in the newborn. *Acta Paediatrica Scandinavica*, 61(5), 571–576.
- Piper, D. W., & Fenton, B. H. (1965). Ph stability and activity curves of pepsin with special reference to their clinical importance. *Gut*, 6(5), 506–508.
- Poquet, L., & Wooster, T. J. (2016). Infant digestion physiology and the relevance of *in vitro* biochemical models to test infant formula lipid digestion. *Molecular Nutrition and Food Research*, 60(8), 1876–1895.
- R Core Team. (2014). R: A language and environment for statistical computing. In R Foundation for Statistical Computing). Vienna, Austria.
- Roman, C., Carrière, F., Villeneuve, P., Pina, M., Millet, V., Simeoni, U., et al. (2007). Quantitative and qualitative study of gastric lipolysis in premature infants: Do mct-enriched infant formulas improve fat digestion? *Pediatric Research*, 61(1), 83–88.
- Russell, A., Canaan, S., Eglhoff, M. P., Riviere, M., Dupuis, L., Verger, R., et al. (1999). Crystal structure of human gastric lipase and model of lysosomal acid lipase, two lipolytic enzymes of medical interest. *The Journal of Biological Chemistry*, 274(24), 16995–17002.
- Sams, L., Paume, J., Giallo, J., & Carriere, F. (2016). Relevant ph and lipase for *in vitro* models of gastric digestion. *Food & Function*, 7(1), 30–45.
- Shani-Levi, C., Alvito, P., Andrés, A., Assunção, R., Barberá, R., Blanquet-Diot, S., et al. (2017). Extending *in vitro* digestion models to specific human populations: Perspectives, practical tools and bio-relevant information. *Trends in Food Science & Technology*, 60, 52–63.
- Signer, E., Murphy, G. M., Edkins, S., & Anderson, C. M. (1974). Role of bile salts in fat malabsorption of premature infants. *Archives of Disease in Childhood*, 49(3), 174–180.
- Yang, Y., Sanchez, D., Figarella, C., & Lowe, M. E. (2000). Discoordinate expression of pancreatic lipase and two related proteins in the human fetal pancreas. *Pediatric Research*, 47(2), 184–188.
- Zoppi, G., Andreotti, G., Pajno-Ferrara, F., Bellini, P., & Gaburro, D. (1973). The development of specific responses of the exocrine pancreas to pancreozymin and secretin stimulation in newborn infants. *Pediatric Research*, 7(4), 198–203.